ライナックの大電流マルチバンチ加速におけるビーム負荷補償と調整法

BEAM-LOADING COMPENSATION AND COMMISSIONING METHOD FOR LINAC WITH HIGH-BEAM CURRENT MULTI-BUNCH BEAM ACCELERATION

栗木雅夫 *A)、金野瞬 A)、リプタック ザカリー A) 高橋徹 A)、大森恒彦 B)、横谷馨 *C)、福田将史 C)、浦川順治 D)
Masao Kuriki*A), Shun KonnoA), Zachary LiptakA), Tohru TakahashiA), Tsunehiko OmoriB), Kaoru YokoyaC), Masafumi FukudaC), Junji UrakawaD)
A)Hiroshima University ADSE
B)KEK IPNS
C)KEK Accelerator Lab.
D)KEK International D.

Abstract

ILC (International Linear Collider) is an e+ e- linear collider based on super-conducting accelerator. In a linear collider, electron and positron pass through the interaction point only once and a large amount of particle per second is required. In the electron driven ILC positron source, positron is captured and accelerated in a multi-bunch format with a high beam loading current. In the linac, the beam loading current and the bunch phase on RF are dynamically changed and the conventional method of the beam loading compensation does not work at all. We propose to introduce detuning on the accelerating cavity to revive the beam loading compensation. We discuss also the tuning method of the linac.

1 . INTRODUCTION

ILC (International Linear Collider) [1] is an e+e- linear collider based on super-conducting accelerator with CME from 250 to 1000 GeV. It would be constructed in Iwate, Japan, as the main project of High energy physics. In the E-driven ILC positron source, the positron is generated in a macro-pulse with 6.15 ns bunch spacing [2] with a normal conducting accelerator to relax the heat load on the positron production target. Because the macro pulse is a copy of a part of DR (Damping Ring) fill pattern, there is a gap as shown in Fig. 1. Seimiya performed a start-to-end simulation of the E-Driven ILC positron source without the beam loading effect [3]. Nagoshi perform the simulation with the beam loading effect [4–6]. To accelerate the beam in such format, the transient beam loading effect which varies the accelerating field at the macro pulse and every mini-train heads, has to be compensated. In Nagoshi's

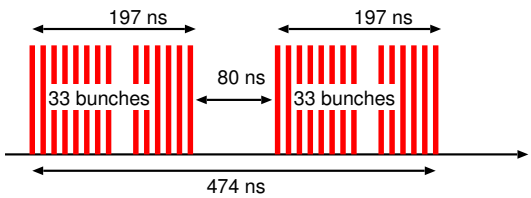

Figure 1: An example of macro-pulse structure in E-Driven ILC positron source. The macro pulse is composed from two mini-trains of 33 bunches with 6.15 ns bunch spacing. There is a gap of 80 ns.

study, we introduce AM (Amplitude Modulation) to control the beam loading effect. In an ideal case where we assume an infinite band width of AM, the transient beam loading (voltage fluctuation over the bunches) can be perfectly corrected. By assuming a finite bandwidth, the effect is reasonably corrected. Unfortunately, this is true only for a crest acceleration, i.e. the bunch sits on the crest of the RF curve. In that case, the voltage by the input RF and the voltage by the beam are in the same phase (or just opposite) and the cancellation between them are simple. If the acceleration is off crest, i.e. the bunch sits off crest of the RF curve, these voltages have a finite angle and cancellation is not simple. The capture linac (the first linac after the positron production target) is the case. The positron is placed at the deceleration phase of the RF and slips down to acceleration phase over the linac. This is the process of positron capture, a kind of bunching. In this process, the bunch phase and the beam loading current are changing. In this case, the simple beam loading compensation does not work at all as we will see later.

In this article, we propose a new beam loading compensation method for a SW (Standing Wave) linac with a high beam loading in off crest acceleration. We performed a simple simulation to confirm the method. At last, we discuss also the tuning method.

2 . THE BEAM LOADING COMPENSATION FOR A SW LINAC OFF CREST ACCELERATION

In this section, we discuss how compensated the beam loading in SW linac off crest acceleration. In the ILC positron source, the acceleration cavity is $\pi/2$ APS (Alternate Periodic Structure) cavity, but it can be treated as a π mode cavity. A cavity is composed from 11 cells (one cell means one acceleration cell and one coupling cell). If we assume the cavity as a big cell (single cell model),

* mkuriki@hiroshima-u.ac.jp

the voltage evolution $V(t)$ with a constant beam loading I is [7],

$$V(t) = \frac{2\sqrt{\beta P_0 r L}}{1+\beta}\left(1 - e^{-\frac{t}{T_0}}\right) - \frac{rIL}{1+\beta}\left(1 - e^{-\frac{t-t_b}{T_0}}\right), \tag{1}$$

where P_0 is the input RF power, r is shunt impedance, L is length of the tube, β is the coupling beta, t is time, t_b is time to start acceleration, T_0 is defined as $T_0 = 2Q/\left[\omega(1+\beta)\right]$, where Q is Q-value and ω is angular frequency of RF. Because the time constant of the input RF and beam loading terms are same, the voltage can be flat if we choose an appropriate t_b as

$$t_b = -T_0 \ln\left(\frac{I}{2}\sqrt{\frac{rL}{\beta P_0}}\right). \tag{2}$$

If this condition is satisfied, the acceleration voltage is flat during the acceleration. The voltage $V(t)$ becomes a constant as

$$V = \frac{2\sqrt{\beta P_0 r L}}{1+\beta}\left(1 - \frac{I}{2}\sqrt{\frac{rL}{\beta P_0}}\right). \tag{3}$$

If the beam and the input RF has a finite angle other than π, the equation (1) is modified as

$$V(t) = \frac{2\sqrt{\beta P_0 r L}}{1+\beta}\left(1 - e^{-\frac{t}{T_0}}\right)\cos(\omega t) - \frac{rIL}{1+\beta}\left(1 - e^{-\frac{t-t_b}{T_0}}\right)\cos(\omega t + \theta), \tag{4}$$

where θ is the bunch phase. In this case, if the amplitude of each terms are adjusted giving a constant of the scalar sum of them, the acceleration field is changed over the pulse as shown in Fig. 2. This is a phase diagram of field in a cavity. The input RF and the beam has a finite angle θ (off crest). At the first bunch, only the input RF field exists (vector $\boldsymbol{A}$). When the beam loading voltage is grown as vector $\boldsymbol{B}$, the input RF is also increased as vector $\boldsymbol{C}$. The acceleration voltage (sum of $\boldsymbol{B}$ and $\boldsymbol{C}$) is vector $\boldsymbol{D}$. The acceleration field is moving from $\boldsymbol{A}$ to $\boldsymbol{D}$. We can adjust the real part (acceleration field strength) of the field, but the phase is moving which has a significant impact on the bunching.

One way to revive the beam loading compensation for the off crest acceleration is both amplitude and phase modulations for the input RF, but it is too complicated because the condition is different for each cavity and it is not so easy to know the beam current and phase.

We propose to introduce the detuning instead of any complicated phase control on RF. The detuning angle ψ is defined as

$$\psi \equiv \tan^{-1}\left(Q\frac{2\Delta\omega}{\omega_0}\right), \tag{5}$$

where $\Delta\omega$ is the detuning angular frequency of the cavity. In this case, the voltage induced by the input RF has the angle, ψ because the cavity has an imaginary component on the shunt impedance, depending on the detuning. That is also true for the beam loading. The voltage induced by the beam has the same angle from the beam phase. If the RF and beam sit on a same phase, the phase diagram is modified as shown in Fig. 3. In this case, the input RF and the beam sit on the same phase. The induced voltage by the input RF, vector $\boldsymbol{A}$ has a finite angle ψ determined by the detuning. The beam loading voltage is grown as vector $\boldsymbol{B}$ on the same phase as the input RF, but the opposite sign. If the input RF is increased as vector $\boldsymbol{C}$, the sum of these field giving the acceleration field can be same as $\boldsymbol{A}$. Note that the beam is accelerated by vector $\boldsymbol{A}$ with the phase ψ, i.e. off crest acceleration.

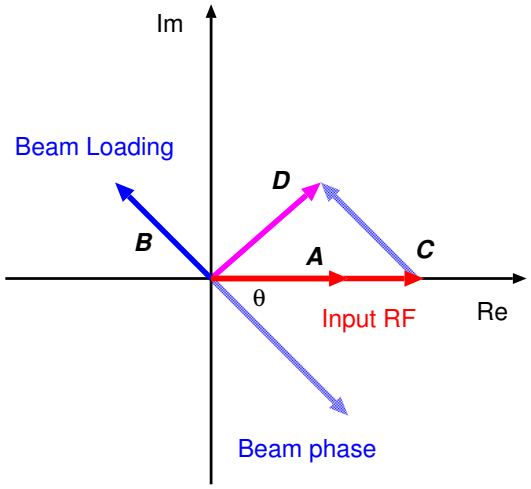

Figure 2: Phase diagram of field in a cavity. In this case, the input RF and the beam has a finite angle θ (off crest). At the first bunch, only the input RF field exists (vector $\boldsymbol{A}$). When the beam loading voltage is grown as vector $\boldsymbol{B}$, the input RF is also increased as vector $\boldsymbol{C}$. The acceleration voltage (sum of $\boldsymbol{B}$ and $\boldsymbol{C}$) is vector $\boldsymbol{D}$. The acceleration field is moving from $\boldsymbol{A}$ to $\boldsymbol{D}$.

In this method, the beam and the input RF are always in phase, but the acceleration phase (the bunch phase on the acceleration field) is controlled by the detuning angle ψ. If t_b is adjusted according to Eq. (2), the acceleration field over the pulse becomes a constant including the phase.

3 . THE POSITRON CAPTURE SIMULATION

In this section, we show the results of the simulation. The simulation performed in three steps. At first, the positron generation is simulated by GEANT4 [8]. The electron beam energy is 3.0 GeV and the W target thickness is 19 mm. The beam size on target is 2.0 mm in RMS. The number of electron on the target is 1000. Generated particles including both electron and positron are the input to the next simulation by GPT [9]. In this step, the tracking simulation over the capture linac was performed. Up

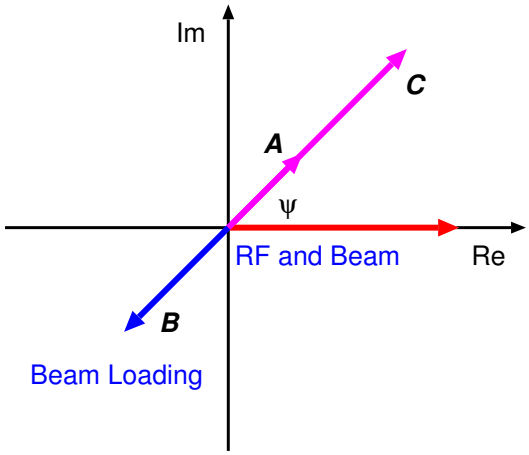

Figure 3: Phase diagram of field in a cavity. The input RF and the beam sit on the same phase. The induced voltage by the input RF, vector $\boldsymbol{A}$ has a finite angle ψ determined by the detuning. The beam loading voltage is grown as vector $\boldsymbol{B}$ on the same phase as the input RF, but the opposite sign. If the input RF is increased as vector $\boldsymbol{C}$, the sum of these field giving the acceleration field can be same as $\boldsymbol{A}$. Note that the beam is accelerated by vector $\boldsymbol{A}$ with the phase ψ, i.e. off crest acceleration.

to this point, the simulation was done with a single bunch. Figure 4, 5 and 6 show the evolution of the longitudinal phase space distribution of positron in the linac. The phase space is defined as z, relative longitudinal position to the bunch center, and δ, the relative energy defined as

$$\delta = \frac{\gamma - \bar{\gamma}}{\bar{\gamma}} \tag{6}$$

where γ is Lorentz gamma factor. As shown in Fig. 4, positron distributed in a narrow region in z with a large energy tail. Because the positron is placed at the deceleration

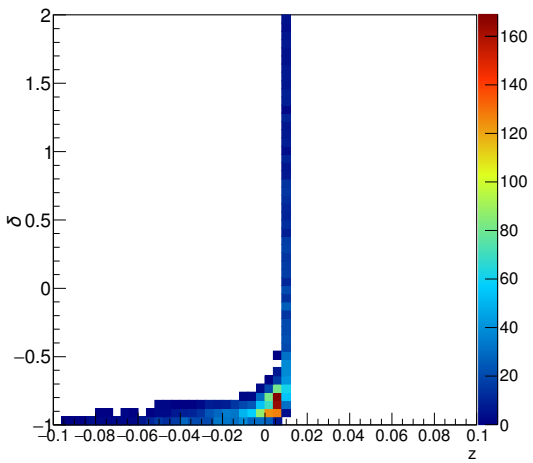

Figure 4: Longitudinal phase space distribution of positron at the beginning of the capture linac.

phase at the beginning of the capture linac, their energy is once decreased and the position is moved to behind towards to the acceleration phase gradually as shown in Fig. 5. In Fig. 6, the positron is further moved to the acceleration phase. The phase space distribution at the exit of the

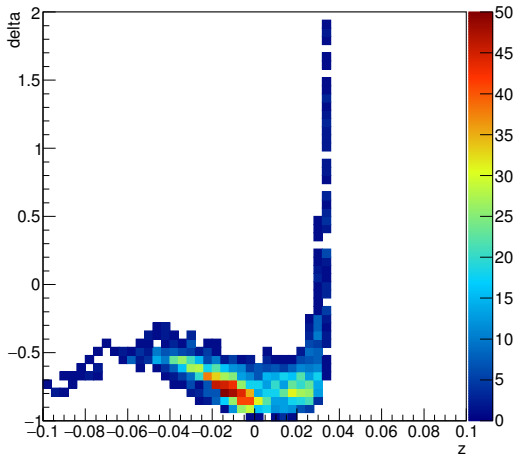

Figure 5: Longitudinal phase space distribution of positron at the middle of the capture linac.

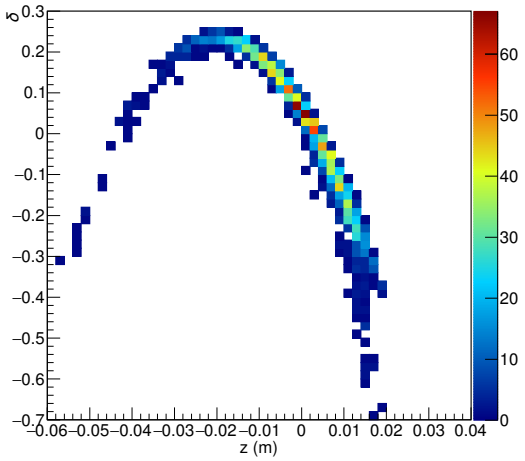

Figure 6: Longitudinal phase space distribution of positron at the exit of the capture linac.

capture linac is shown in Fig. 6. The positron is captured in a RF bucket, but distributed along a large phase region. The beam passes through the chicane before the acceleration by the booster. The primary purpose of the chicane is removing the electron, but the side effect is bunching. For that purpose, R_{56} of the chicane is adjusted as 0.053. The phase space distribution after the chicane is shown in Fig. 7. The dense part of the positron distribution is aligned vertical direction resulting a smaller z distribution which decrease the energy spread after the acceleration by the booster as shown in Fig. 8. In the booster acceleration,

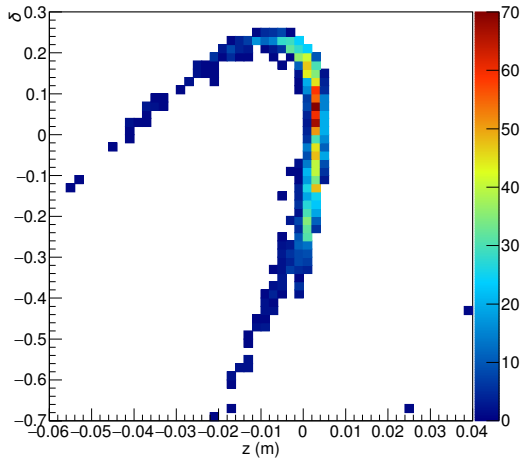

Figure 7: Longitudinal phase space distribution of positron after the chicane at the downstream of the capture linac.

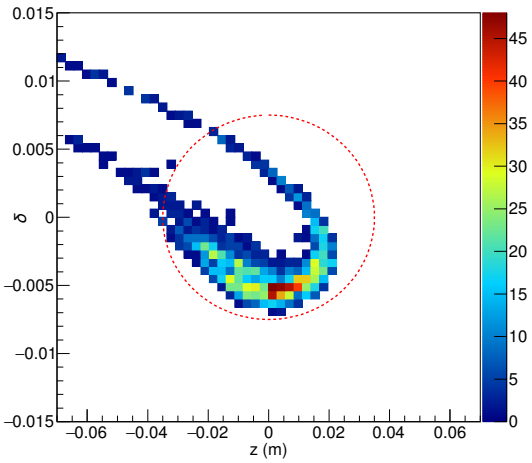

Figure 9: Longitudinal phase space distribution of positron at the last part of the capture linac.

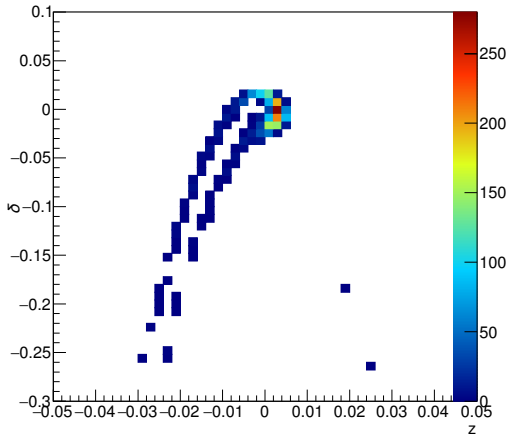

Figure 8: Longitudinal phase space distribution of positron at the last part of the capture linac.

the most dense part of the distribution is placed at the crest of the RF field. A long tail along the RF curve is seen in Fig. 8.

The positron is finally injected and stored in DR (Damping Ring) to make up the beam shape as a extremely small vertical emittance to improve the luminosity. Dynamic aperture of DR gives the acceptance for the positron as

$$\gamma A_X + \gamma A_y < 0.07 \tag{7}$$

$$\frac{z^2}{0.035^2} + \frac{\delta^2}{0.0075^2} < 0.015. \tag{8}$$

z distribution in Fig. 8 can fit to the acceptance, but δ distribution does not. ECS (Energy Compressor Section) composed from Chicane and RF section adjusted the distribution. R_{56} and R_{65} of the sections are 1.14 and -0.90, respectively. The distribution after ECS is shown in Fig. 9. The dashed circle shows the DR acceptance in the space. The positron in the acceptance is "captured" and the yield of the positron per electron is defined as the ratio of the number of the captured positron per the number of electron on target. In this study, only the longitudinal phase space is considered to evaluate the yield.

4. BEAM LOADING COMPENSATION WITH THE DETUNING

The study up to now is performed as the single bunch, but the beam loading current and the beam phase with respect to the RF field can be evaluated as shown in Fig. 10 and 11. In both, the solid line shows the total, the dashed line shows that by positron , and the dotted line shows that by electron. In phase calculation, the average is taken the positron phase and the inverse of electron. The beam loading current is obtained as

$$I = \sum \frac{q_i \beta_i}{2 t_{bunch}} \sqrt{A^2 + B^2} \sin\left[\omega t + \frac{\omega}{\beta_i c}(z_1 - z_i) + \phi_0 + \theta\right], \tag{9}$$

where q_i is charge of particle, t_{bunch} is bunch spacing, β_i is Lorentz beta for each particle, z_i is the position of particle, z_1 is the entrance position of cavity, ϕ_0 is the initial phase of RF, c is speed of light, θ is obtained as

$$\theta = \sin^{-1} \frac{B}{\sqrt{A^2 + B^2}} \tag{10}$$

where $A = (1 - \cos \pi/\beta_i$ and $B = \sin \pi/\beta_i$. By using these data, the beam loading field for each bunch is obtained. By integrating the field, the energy modulation with respect to the first bunch is obtained. The energy after the capture linac as a function of bunch index is shown in Fig. 12. t_b for each cavity is adjusted as Eq. (2), but the

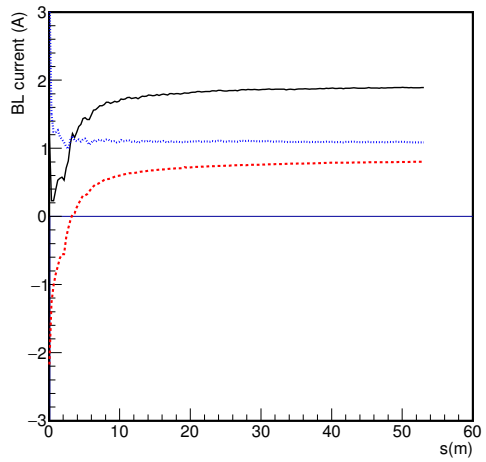

Figure 10: Beam loading current as a function of the longitudinal position s. The origin is the downstream end of the target. The solid line shows the total current, the dashed line shows the positron current, and the dotted line shows the electron current.

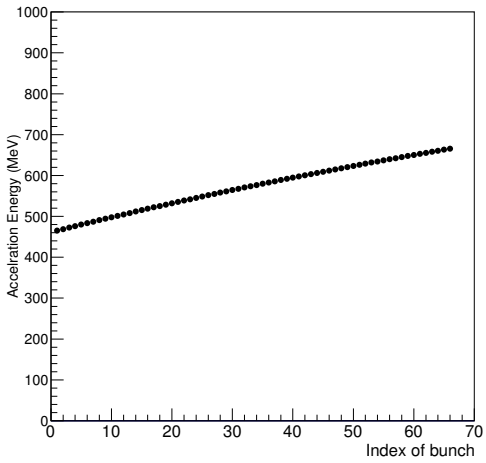

Figure 12: Energy after the capture linac as a function of bunch index (from the first bunch to the last bunch) is shown.

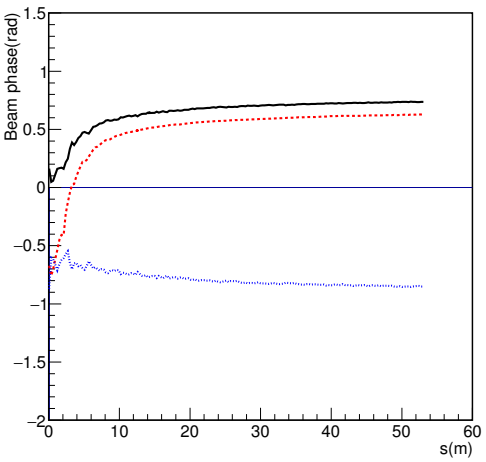

Figure 11: Beam phase with respect to RF field (rad) as a function of the longitudinal position s. The origin is the downstream end of the target. The solid line shows the phase of all beam, the dotted line shows the phase of positron, and the dotted line shows the phase of electron.

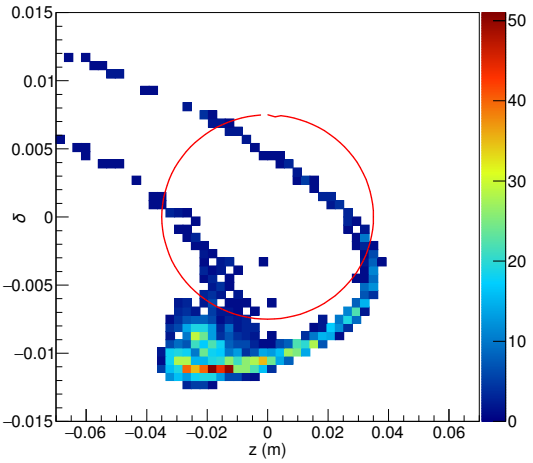

Figure 13: The phase space distribution after ECS of the 20th bunch.

energy is not flat at all as we expected. The yield for those bunches is much spoiled comparing to the first bunch. For example, the phase space distribution of the 20th bunch at the exit of ECS is shown in Fig. 13. Due to the energy shift, the most of positrons is not in the acceptance.

Figure 14 shows the yield as a function of bunch index. The yield is kept only the first several bunches, and then rapidly decreased and almost zero after the 20th bunch due to the beam loading effect with a finite phase.

To cure this problem, the compensation with the detuning was tried. In principle, we should set the different tuning angle for each cavity depending on the beam loading phase as shown in Fig. 11, but it is hard to know the phase in a real operation. Instead, we set a global detuning phase over the linac. There are two reason,

(a) Except the first part of the linac, the phase is almost constant as shown in Fig. 11.
(b) In the first cavity, which is very important for the capturing (bunching), the beam loading current is almost zero, because the positron and electron are in a same position. The current by the positron and electron cancels each other.

Figure 15 shows the yield as a function of bunch index, for various detuning angle; 0 to 0.81 rad with 0.09 rad step. The legend is diamond (0 rad), solid square (0.09 rad), solid triangle(0.18 rad), inverse solid triangle (0.27

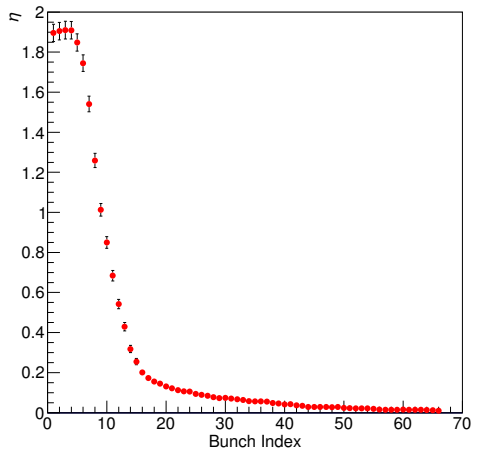

Figure 14: The yield as a function of the bunch index with a conventional beam loading compensation, i.e. zero detuning.

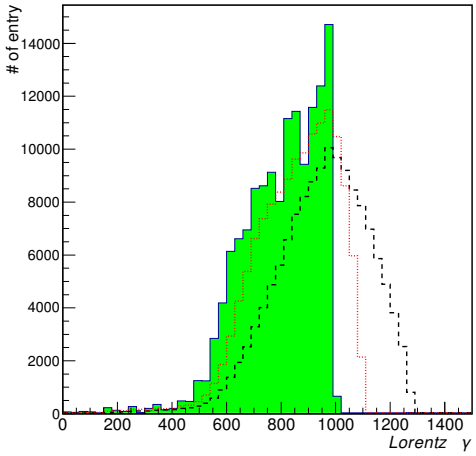

Figure 16: Histogram of Lorentz γ after the chicane at the down stream the capture linac. Filled histogram is by 0.63 rad detuning, that by the dashed line is by 0 detuning, and that by the dotted is 0.36 rad detuning.

rad), open circle (0.36 rad), open square (0.45 rad), open triangle (0.54 rad), solid circle (0.63 rad), open cross (0.72 rad), and solid star (0.81 rad). Among them, 0.63 rad gives the best result and the yield over the pulse for each bunch is constant within the statistical error.

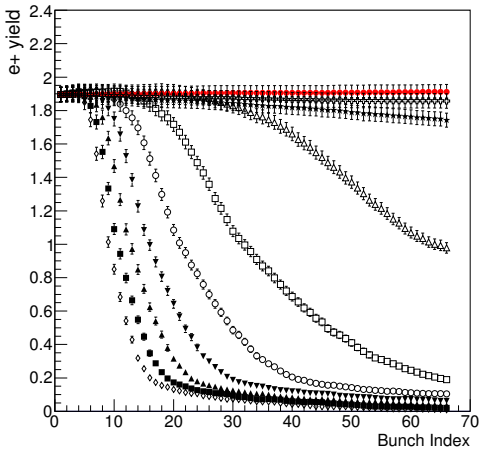

Figure 15: The yield as a function of bunch index with various detuning angle. The legends are diamond (0 rad), solid square (0.09 rad), solid triangle(0.18 rad), inverse solid triangle (0.27 rad), open circle (0.36 rad), open square (0.45 rad), open triangle (0.54 rad), solid circle (0.63 rad), open cross (0.72 rad), and solid star (0.81 rad).

To observe the detuning effect more clearly on the kinematics, Lorentz γ and z is observed after the chicane at the down stream of the capture linac. The histogram with the solid are is 0.63 rad detuning, that with the dashed line is 0 detuning, and that by the dotted line is 0.36 rad detuning. In both figures, the distribution by the 0.63 rad

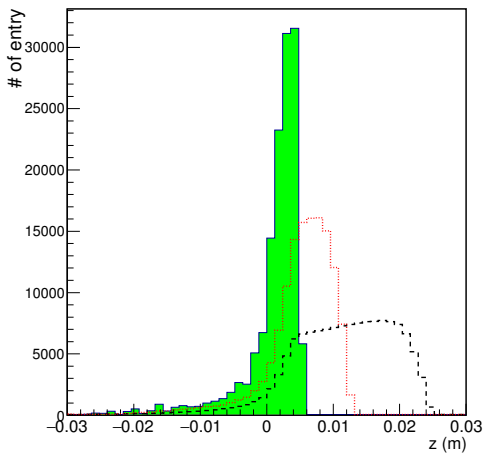

Figure 17: Histogram of z after the chicane at the down stream of the capture linac. Filled histogram is by 0.63 rad detuning, that by the dashed line is by 0 detuning, and that by the dotted is 0.36 rad detuning.

detuning shows narrow peak, especially on z distribution. That means that the phase space distribution of each bunch is well adjusted by the global detuning over the linac. That is the reason that the yield is constant as shown in Fig. 13.

5. TUNING METHOD FOR THE CAPTURE LINAC

We start the tuning with the single bunch case. The phase of each cavity is a global parameter, i.e. all cavity is set to the same phase, θ. If the spacing between the cavity is odd number of the half wavelength of the RF wave, the phase should be opposite, i.e. $-\theta$. In this step, tuning

parameter is only the phase θ. We choose the best θ giving, e.g. the least z distribution after the chicane, the least Lorentz γ distribution after the booster, etc. Once we tuned the capture linac, we can set t_b for each cavity according to the beam loading current. Although the exact beam loading current can't be measured with a precise resolution, we can estimate it according to the simulation. The beam loading current of the first cavity is zero. The beam loading curent of the cavity later than the second cavity is almost a constant. The beam loading of the second cavity is almost half of the constant. Therefore, all we have to do is to fix one parameter in this step, the beam loading current for the cavity later than the second. Once t_b is determined, the number of bunches in a pulse is increased. In this condition, the detuning angle ψ should be increased to minimize z distribution after the chicane. In this process, the acceleration angle ϕ, sum of θ and ψ should be constant as

$$\phi = \theta + \psi. \tag{11}$$

Finally, θ becomes zero and ψ take over the initial value of θ. The tuning can be independent from the beam current, but the effect is proportional to the beam current. Repeating the tuning of θ, t_b and ψ, we will arrive at the promised land. In the process, the bunch number and charge can be gradually increased. The bunch number does not change the parameter at all, but the bunch intensity change t_b, according to Eq. (2).

6 . SUMMARY

We discuss the beam loading compensation of a linac with the SW cavities in case of off crest acceleration. By introducing the cavity detuning, the beam loading can be compensated, as same as in the case of crest acceleration. The method is examined for the capture linac of ILC positron source and the positron yield can be constant over the 66 bunches by the global detuning method. Because the tuning parameter is global, i.e. same for all cavity except t_b, the tuning scenario is very simple and does not require any precise beam diagnostics for each cavity. The result is based on very simple simulation considering only longitudinal kinematics after the capture linac. The next issue is to confirm the conclusion with a more realistic simulation.

ACKNOWLEDGEMENTS

This work is partly supported by Grant-in-Aid for Scientific Research (B) and US-Japan Science and Technology Cooperation Program in High Energy Physics.

REFERENCES

[1] ILC Technical Design Report, KEK-Report 2013-1(2013).
[2] T. Omori *et al.*, Nucl. Instr. and Meth. A**672**, 52(2012).
[3] Y. Seimiya *et al.*, Prog. Theor. Exp. Phys. 103G01(2015).
[4] M. Kuriki *Proc. of LINAC2016*,TUPRC008(2016).
[5] H. Nagoshi *et al.*, Nucl. Instr. and Meth. A **953** 163134 (2020).
[6] S. Konno *et al.*, *Proc. of PASJ An. meeting 2020*, FRPP66 (2020).
[7] P. B. Wilson, SLAC-PUB-2884(1982).
[8] GEANT4; `geant4.web.cern.ch`
[9] General Particle Tracer, Pulsar physics; `pulsar.nl/gpt/`